

Mineral equilibria in silicate and ore systems

#Lebedev E.B., Kadik A.A., Kononkova N.N. Experimental study of the mechanisms of metallic, sulfide and silicate phases separation at definite degrees of melting of the system. (a simulation with the help of a high-temperature centrifuge)

GEOKHI RAS elkor@geokhi.msk.su

At the early stages of formation of planetary bodies, silicate, metallic, and sulfide phases, which have been formed in the course of the partial or complete fusion of the initial planetary substance, were subjected to a gravitational differentiation.

It is assumed that sulfur is one of the major elements entering the composition of metallic cores of the Earth and the Moon.

The goal of this study is to conduct, using a high-temperature centrifuge, the experimental simulation of the gravitational differentiation of a partially molten sulfide- and metal containing silicate substance → the olivine → basalt mixture, which can be considered, in a first approximation, as a model of the planetary substance. Our main objectives are: (i) to elucidate the mechanisms of the separation of metallic and sulfide phases from the silicate crystalline matrix and the accumulation of these phases at different degrees of melting of the silicate substance; (ii) to determine the possibility of the formation of an independent layer of the metallic and sulfide phase by means of its percolation through the crystalline matrix; (iii) to apply the results of the study to the solution of problems of chemical differentiation of the Moon and other planetary bodies in the thermal and gravitational fields.

A simulation of the migration and accumulation of metallic (Fe) and sulfide phases (FeS) under gravity, with the partial fusion of a model planetary substance (olivine → basalt mixture), is carried out in a high-temperature centrifuge. The separation and motion of metal and sulfides in the intercrystalline space is shown to be in an intimate relationship with the degree of fusion of a silicate material. If the fraction of the silicate melt present in the space between the olivine crystals exceeds 5-10 vol.%, this quantity is enough to produce a set of mutually related channels between the grains, through which a percolation of silicate, metallic and sulfide liquids becomes possible. Droplets of the sulfide melt do not mix with the silicate melt and can move along the silicate intergranular channels under the influence of gravity. Thus, the mixture consisting of olivine crystals, silicate, metallic and sulfide melts, after being separated in a centrifuge, is differentiated in density. As a result, the metallic, sulfide and silicate phases are divided into independent layers.

The studies were supported by the Russian Foundation for Basic Research (project codes nos. 97-05-64786, 98-05-064768, and 99-05-65479)

In the SC- 8 specimen (67.5 vol.% 01, 22,5 vol. % Bas, 10 vol.% FeS) containing -23 vol % of the silicate melt, a sharply irregular height distribution of phases is observed. The following main zones are distinguished in the vertical section of the specimen. The top zone (A) of the floated-up basalt melt, represented by glass and quenched pyroxene crystals, does not contain olivine crystals and sulfide globules. The central zone (C), which forms the main part of the specimen, predominantly contains olivine crystals in amounts of 85-90 vol.% (crystalline matrix) with the silicate melt (glass) among them. The width of the intergranular channels ranges from 3 to 30 pm. In the lower part of this zone, in basaltic glass (as a rule, in the central parts of the channels), fine sulfide globules up to 1 pm in size are located. The sulfide content in this zone does not exceed 1-3 vol%o. Between the top (A) and central (C) zones of the specimen, a narrow transition zone (B) is observed, in which olivine crystals abruptly replace the glass of the basalt melt. The lower, near- bottom zone (D) of the specimen completely consists of iron sulfide - pyrrhotine, which was formed from the sulfide liquid at the instant of specimen quenching.

The observed distribution of phases over the height of the SC-8 specimen clearly demonstrates the result of the gravitational differentiation of the substance: the segregation of phases in density. Under the influence of gravity, the sulfide phase easily percolates (is filtered) through the crystalline matrix along the intergranular channels and is almost completely accumulated in the near-bottom part of the specimen in the course of the experiment. In the central part, only an insignificant sulfide portion is retained in the form of very fine globules (drops), which had no time to settle down. Clearly, the filtration of the silicate liquid occurs in the opposite direction - into the top part of the specimen, where a layer of pure melt is formed.

In the SC -12 specimen (60 vol.% 01, 20 vol. % Bas, 10 vol.% Fe, 10 vol% FeS) a sharply irregular height distribution of phases is observed. The following main zones are distinguished in the vertical section of the specimen. The top zone of the floated-up basalt melt is represented by glass and quenched pyroxene crystals. The central zone (C), which constitutes the main part of the specimen, predominantly contains olivine crystals in amounts of 85 — 90 vol.% (crystalline matrix). In the lo'A'cr part of this zone, in basaltic glass (as a rule, in the central parts of the channels), fine sulfide globules, containing iron globules, are located. The lower, near-bottom zone (D) of the specimen consists of iron sulfide - pyrrhotine, containing iron globules.

The results of the experiments have shown that the mixture consisting of, olivine crystals, a basaltic silicate melt, an iron and an iron sulfide melts, after being subjected to centrifuging, is differentiated in density only at definite degrees of melting of the silicate substrate.

In this work we carried out, with the help of a high-temperature centrifuge, the simulation of the processes of the accumulation and migration of metallic and sulfide

phases corresponding to the partial melting of the model substance in the planet's interior. Experiments led us to conclude that the separation of metallic and sulfide phases and their motion in the intercrystalline space are in a close relationship with the degree of the mantle fusion. The mixture of olivine crystals, a silicate basaltic melt, and a metallic and sulfide melt, subjected to centrifugal separation, is differentiated in density. As a result, the iron, iron-sulfide and silicate phases are separated into independent layers.

#Ezhov S.V. On the significance of diffusion transport of components while processes of localization of eutectic smeltings.

Moscow State Geological Prospecting Academy,
Miklukho-Maklai str., 23, Moscow, 117873 Russia

key words [eutectic diffusion sulfides melts bimetasomatism experiments]

Formation of large melt amounts while continuous rock anatexis is not difficult to understand - the only need is sufficient heating to make the rock matter melted. In case of partial fusion the problem is more complicated. Melted phase in the mineral mixture appears as films and drops. Large isolations of eutectic composition are forming as a result of merging of small ones. To explain such a merging assumptions of pressing-filter (expression of melts out of low pressure areas) or gravity sedimentation are taken into account. Our recent experiments suggest one more mechanism that can explain various natural phenomena.

The sulfide eutectic (PbS+Cu₂S) that is quite handy because of low temperature (550°C) was under modeling. The experimental matter contained both silicate (granodiorite-porphry) and carbonate (limestone and dolomite) rock. Ore components were introduced as a barley mixture of galena, chalcopyrite, and sphalerite. The

preparations were heated up to 550-600°C at 1 kbar pressure in the presence of NaCl and KCl water fluid.

The eutectic fusion takes place in two locations:

1 - in situ, replacing initial components among sulfide minerals clumps. The fusion fills the intergrain space.

2 - in the places far from initial layout of components. The fusion looks like drops of various dimension with characteristic inner morphology (fig. 1). They were located both on the carbonate rock surface that are in contact with chloride fluid, and in the area of bimetasomatic skarn columns parallel to their borders (fig. 2). In the last case were combined into long-shaped lens microdeposits. The surface carbonate rock drops made up to a layer 1 mm thick. A distinct distribution of the drops' dimension through the thickness was marked. The smallest of them are sited directly at the carbonate rock surface, and going aside their dimensions are rapidly increasing. It is obvious that melt formation is evolving simultaneously to the limestone dissolution: the drops' nucleation takes place on the surface of kaolonite and calcite grains. Henceforth, while calcite dissolution, the growing drops located at some distance from the border of carbonate rock.

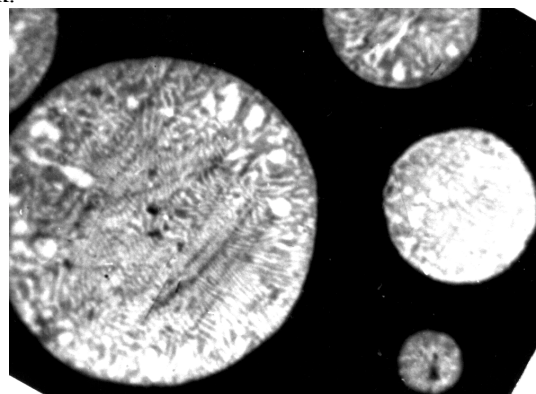


Fig. 1. Drops of sulphide eutectic.

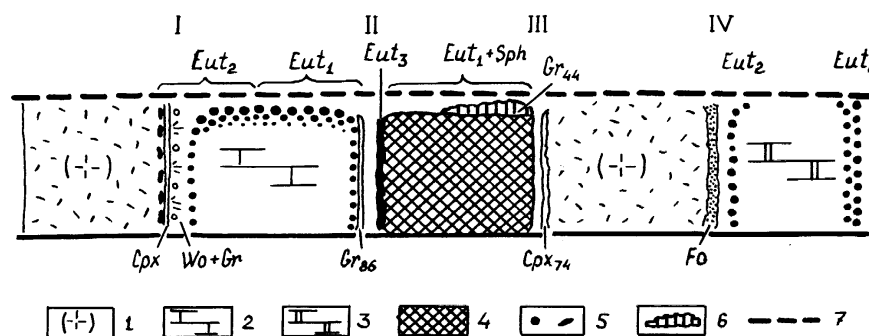


Fig. 2. Scheme of sulphide meltings location within specimen structure. Experiment AT-93. 1 – granodiorite-porphry, 2 – limestone, 3 – dolomite, 4 – mixture of galena, sphalerite and chalcopyrite (before the experiment realisation), 5 – sulphide melt segregations, 6 – garnet on the sulphide ore surface, 7 – perforated side of ampule where the specimen had free contact with open solution. Nomenclature of minerals: Cpx – clinopyroxene (lower index – hedenbergite share, %), Fo – forsterite, Gr – garnet (index – andradite share, %), Shp – sphalerite, Wo – wollastonite, Eut – sulphide eutectic.

Change in the fusion composition vs its site is detected. The in-situ fusion, as well as the melted drops that are close to its components source, contains 24% of galena and 76% of chalcocite. The drops separated by

more than 6 mm from its source contain 17% and 83% of galena and chalcocite, respectively.

The noted observations show that both melted segregation and crystalline phases could be sited far from

its components' source. The matter migrates not as a melted phase. Components of the future anatexis fusion are in the solute state, and are transported via fluid phase because of diffusion. The only gradient of concentrations is needed – solubility of ore components in place of their initial localisation must be higher than in place of melt formation. The causes of concentration of components as a melt may have either geochemical nature, like in conducted experiments when the melt was concentrated on the surface of limestone or dolomite, or physical one, for example in zones of failed pressure (within open tectonic fissures, interboudin space, etc.). Such nature may have different granitoid smeltings and pedmatite bodies in ultrametamorphism regions, as well as some ore bodies of magmatic genesis.

#Chanturija V.A., Fedorov A.A., Bunin I.J., Zubenko A.V., Nedosekina T.V. Computer images analysis of gold-containing pyrite and arsenopyrite in separation mechanisms and minerals breaking-up investigation

Research Institute of Comprehensive Exploitation of Mineral Resources RAS, Kryukovsky Tupik 4, Moscow 111020; fedorov@ipkonran.ru

key words [*electrophysical properties surface fineness and geometry of mineral particles*]

At processing of the gold-containing ores the authentic information about the character of the gold particles precipitation and about the gold particles association with the mineral matrix is necessary. Also it is necessary to have the data about the structural-morphological parameters of the gold particles and the minerals defects structure.

Earlier the computer images analysis was used to predict the technological properties of the South-Sakhalin gold-quartz ores [1] and to estimate the production possibility of the gold-containing copper concentrate from the deposit Shinchao (China) pyrites tails [2]. Also this method was used for the mineralogical-technological estimation of the rest gold-containing ores and concentrates [3-5]. In the latter case this method was used for the ores and minerals properties prediction, and for the theoretical investigations of the behaviour mechanisms of

This work was supported by the RFFI under Grant № 99-05-65236

the gold-containing sulphide minerals in the flotation and geotechnological processes.

In IPKON RAS to solve the problems of gold-containing pyrites and arsenopyrites separation and of the breaking-up of gold-containing ores the technique of complex estimation of minerals softening is developed. The method of the computer images analysis of minerals surface structures and fine-grained minerals particles structures made a basis for this technique.

For the explanation of the features peculiar of the electrophysical and technological properties of sulphide minerals (pyrite and arsenopyrite) and for the description of computer images of minerals surface defects structures the method of fractal parametrisation of structures is used. This approach to the quantitative analysis of natural disorder allows to assign to each surface defects structure the concrete fractal dimension (D_f). In addition to the traditional statistical methods this method enables to describe the disordered structures of minerals in the strict quantitative terms of fractal geometry.

The fractal dimension of the defects structures of minerals surface local regions, and also their physical properties are given in the Table. For arsenopyrite the negative linear correlation between the normalized values of the specific resistance $\rho^{Ar}/\rho^{Ar}_{max}$ and D_f -values is established, and the positive linear correlation between the thermoEMF ($\alpha^{Ar}/\alpha^{Ar}_{max}$) и D_f is established. Also a linear correlation between ρ^{Ar} и α^{Ar} (for $D_f \geq 1,65$) is obtained: $\rho^{Ar}/\rho^{Ar}_{max} = 1 - 0,8(\alpha^{Ar}/\alpha^{Ar}_{max})$.

The comparison of the separation force of the air bubble from the local sites of mineral surface with the fractal dimension of the surface defects structure has allowed to determine the regions of the surface geometry action on the local hydrophobe properties of pyrite and arsenopyrite. The influence of the surface heterogeneity factor is most actively shown in the range pH 9-11. In this range the fractal dimension D_f determines the distinctions between the force of air bubble from the surface of pyrite and arsenopyrite.

Alongside with the investigations of gold-containing sulphide minerals separation process the computer images analysis was used to the study of gold-containing pyrite and arsenopyrite breaking-up mechanisms under the electrochemical action. In this case both the plain macro-specimens of monominerals units and particles of crushed materials were investigated for the quantitative description of minerals surface structures and for the estimation of particles geometrical characteristics change.

Table. Fractal dimension of defects structures (D_f) and electrophysical characteristics of minerals surface local areas

Mineral	D_f	$\rho \cdot 10^{-3}$, Om·m	$\alpha_{thermoEMF}$, $\mu kV/^{\circ}C$
Pyrite	1,770	12,5	400
	1,695	4,5	450
	1,691	11,0	240
	–	7,5	340
	1,473	6,25	320
Arsenopyrite	1,652	1,86	70
	1,536	3,43	120

	1,861	0,63	160
	1,711	1,64	110
	1,485	1,65	20

The computer images analysis of gold-containing pyrite and arsenopyrite plane grinded-and-polished specimens before and after electrochemical treatment has allowed to study the evolution of minerals surface defects structure under electrochemical action. The microdamages growth process and minerals intergrown pieces borders disclosing process were described. The process of minerals surface softening in time (t) was estimated quantitatively by the change of the fractal dimension ($D_f(t)$) of minerals surface defects structures before and after treatment.

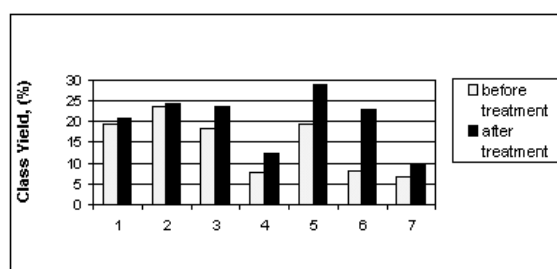


Fig. The histogram of class -0,1mm content (1-5 – pyrites, 6-7 – arsenopyrites).

The analysis of computer images of the Nezhdaninsky gravitation concentrate fine-grained particles before and after electrochemical treatment has shown the class -0,1mm content change (see.Figure). The evolution of the particles form (rounding and form-factor) under the electrochemical treatment was investigated.

Thus, the application of computer images analysis for the decision of minerals processing tasks and technological mineralogy problems allows to predict the behaviour of gold-containing sulphide minerals in the hydrometallurgical processes and also to reveal the separation mechanisms of minerals.

References:

1. Chanturija V.A., Bashlykova T.V., Chanturija E.L. // Mining Journal (Rus.), 1995, № 11. P.46-50.
2. Chanturija V.A., Bashlykova T.V. // Mining Herald (Rus.), 1998, № 1, P. 37-52.
3. Chanturija V.A., Fedorov A.A., Chekushina T.V. et al.//Mining Journal (Rus.),1997,№ 10,C.51-56.
4. Chanturija V.A.,Fedorov A.A.,Bunin I.J.//Doklady Chemical Technol.,1998,V.362,№4,C.513-517.
5. Chanturija V.A., Fedorov A.A., Bunin I.J. et al. // Mining Journal (Rus.), 2000, № 2, P.24-27.

Likhacheva A.Yu., Paukshtis E.A., Miroshnichenko Yu.M. The reaction of thermal decomposition of ammonium analcime

Institute of mineralogy and petrography, pr. ac. Koptuyuga 3, Novosibirsk 630090 alih@uiggm.nsc.ru

key words: [ammonium, analcime, thermal decomposition, IR spectroscopy, dehydroxylation]

To investigate the mechanism of thermal decomposition of natural ammoniumbearing aluminosilicates the ammonium-exchanged form of natural analcime $\text{Na}_{1.83}[\text{Al}_{1.88}\text{Si}_{4.12}\text{O}_{12}]\times 1.97\text{H}_2\text{O}$ (r.Nidym, Siberian platform) was used as a model object. Thermal decomposition of NH_4 -analcime was studied by DTG, gas chromatography and IR spectroscopy at 25-700°C.

The DTG curve of NH_4 -analcime contains one peak between 400° and 700° with maximum at 600° of 12.2% weight loss. According to gas chromatography, in this temperature interval NH_4 -analcime loses 12.3 wt.% of water and 1.5 wt.% of nitrogen. At room conditions the NH_4 -analcime is waterless. Thus we can suppose that at rising temperature water is formed by reaction between the ammonium hydrogen and the framework oxygen - dehydroxylation. This process evidently leads to significant destruction of the framework, due to a large amount of water removed from the sample. The nitrogen formed at the decomposition of ammonium is fixed in the sample and only partially removed at 700°.

IR spectrum of NH_4 -analcime contains at room temperature in the region of 2500-4000 cm^{-1} only absorption bands of NH_4^+ -ion (cm^{-1}): 1430, 3060, 3250 and overtone 2850. The deviation from selection rule for tetrahedral molecule - appearance in the IR spectrum of the band 3060 cm^{-1} (ν_1) and splitting of band 1430 cm^{-1} (ν_4) observed at -160° - evidences for the distortion of the NH_4^+ -ion configuration [1] influenced by hydrogen bonds with the framework oxygen.

The decomposition of NH_4^+ -ions starts at 400° and reaches its half-way at 500°, according to the gradual decreasing of corresponding bands in the IR spectrum (Fig.1). The narrowing of the band 1430 cm^{-1} of bending vibrations of the NH_4^+ -ion at 550° evidences for its geometry to approach the ideal tetrahedron. This is probably related to the changing of its hydrogen bonds with the framework due to the deformation of structural channels.

At $t=550-650^\circ$ the bands 1330, 1625 cm^{-1} of ammonia bonded to Lewis acid sites $\equiv\text{Al}:\text{NH}_3$ [2] are observed in the IR spectrum. These bands increase in intensity with temperature in parallel with decreasing of the NH_4^+ -ion bands intensity, and practically disappear at 700°. The formation of complexes $\equiv\text{Al}:\text{NH}_3$, most probably located in the framework, is caused by several factors. Narrow channels of the analcime structure prevent fast diffusion of ammonia formed at the decomposition of NH_4^+ -ions. At $t > 550^\circ$ the dehydroxylation of the framework proceeds intensively giving rise to Lewis centres - coordinately unsaturated aluminum species. These centres are known to adsorb easily the ammonia molecules to form stable complexes $\equiv\text{Al}:\text{NH}_3$ [3].

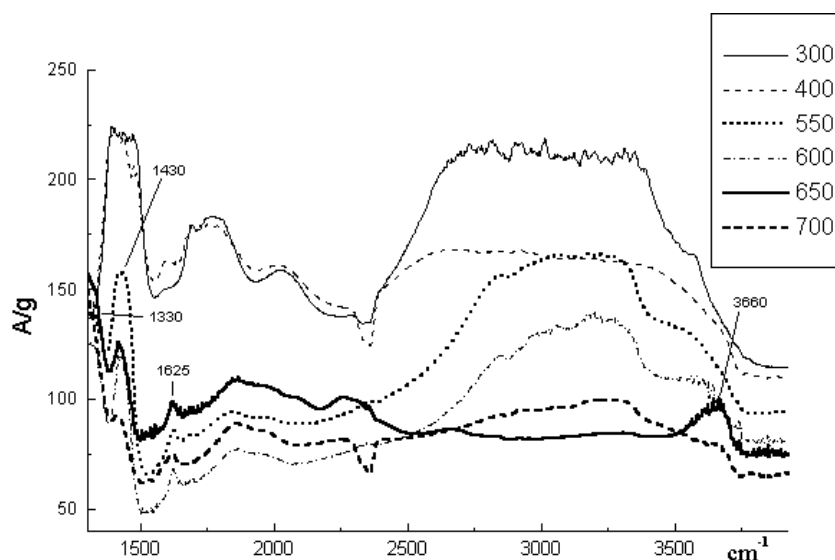


Fig.1. IR spectra of NH_4 -analcime at 300-700°C (A/g - normalized optical density).

A sharp changes of the spectrum in the region of the framework overtone vibrations 1500-2000 cm^{-1} at 550° are probably related to the transformation and starting destruction of the analcime framework, caused by dehydroxylation.

Starting from 550° a shoulder of O-H stretching vibrations in hydroxyl groups appears in the region of 3600 cm^{-1} (Fig.1). As it was suggested, these groups are localized in the framework. As the temperature increases, this shoulder is shifted to high frequencies and decreases in intensity. The band 3660 cm^{-1} observed at 650° seems to correspond to mixed absorption of OH-groups and molecular water.

The decomposition of ammonium and complexes $\equiv\text{Al}:\text{NH}_3$, as well as the removal of water from the sample are almost completed at 700°, according to IR spectroscopy and gas chromatography. The calculation of weight loss in NH_4 -analcime shows that the formation of 12.3 wt.% of water requires complete decomposition of ammonia into nitrogen and hydrogen. Evidently this is the case, as ammonia is unstable at high temperatures. Moreover, the framework "activated" by dehydroxylation seems to catalyze the decomposition of ammonia.

The kinetic diameter of the nitrogen molecule exceeds the diameter of structural channels in the analcime framework by about 1 Å [4]. This is one of the reasons for fixing nitrogen in our sample. We also have to suppose that a part of nitrogen forms chemical bonds with the framework atoms to restore the charges balance disturbed at dehydroxylation when the analcime framework loses one fifth part of the total amount of oxygen.

Thus we can divide the process of thermal decomposition of NH_4 -analcime into several steps:

400° - beginning of decomposition of ammonium on ammonia and protons, formation of the framework hydroxyl groups;

550° - beginning of dehydroxylation, further decomposition of ammonium, formation of complexes $\equiv\text{Al}:\text{NH}_3$, strong deformation of the framework;

600-650° - decomposition of complexes $\equiv\text{Al}:\text{NH}_3$ and ammonia, dehydroxylation with mass removal of water;

700° - completion of decomposition of ammonium and ammonia, destruction of complexes $\equiv\text{Al}:\text{NH}_3$ and dehydroxylation, partial removal of nitrogen.

The peculiarity of the analcime structure - the presence of narrow channels in its framework - causes active interaction of the ammonium decomposition products with the framework leading to its destruction at 700°.

References:

1. Chourabi B, Fripiat JJ, *Clays and Clay Miner.*, **29**, N4, 260-268, (1981)
2. Knozinger H, Kriltlenbrink H, Ratnasamy P, *J.Catal.*, **48**, 436, (1977)
3. Corma A, *Chem.Rev.*, **95**, 559-614, (1995)
4. Breck D., *Zeolite molecular sieves*, M. (1976) (in Russian)

#Chepurov A.A. Experimental study of diamond crystallization in metal - silicate - carbon systems

Design and Technological Institute of Monocrystals SB RAS ,
Russkaya str., 43 , Novosibirsk 630390 chepurov@ns.nsi.ru

key words: [diamond, synthesis, experiment, silicate, metal]

The existing mineralogical and experimental data allow to conclude, that most of natural diamonds were formed in the ancient Earth mantle, where highly reductive conditions provided stability of the transition metals in their free state. Thus one can assume, that diamond crystallization proceeded from heterogeneous substrates of silicate-metal-carbon, silicate-sulphide-metal-carbon or more complex composition.

The work was done with the financial support of the RFBR (project 99-05-64687).

We have conducted experimental modeling of the process of diamond crystallization in the system metal (Fe,Ni alloy) - silicate (basalt melt or solid olivine) - carbon. The experiments were held on the multi-anvil high-pressure apparatus "BARS" [1]. The source of carbon was placed in the central, the most high-temperature zone of the high-pressure cell; above it, the metal-silicate schist and a diamond crystal seed were put. The carbon source was graphite, while for seeds, synthetic diamond crystals 0,3 mm in size served. The metallic content of the schist was a mixture of iron and nickel with the ratio Fe:Ni = 3:7. For added silicates, synthetic olivine of the following composition (wt. %): SiO₂ - 31,11; TiO₂ - 0,07; Al₂O₃ - 0,04; Cr₂O₃ - 0,01; FeO - 62,42; CaO - 4,70; MgO - 3,33; MnO - 0,15, and natural glass with alkaline basaltic composition: SiO₂ - 46,60; TiO₂ - 2,24; Al₂O₃ - 15,27; Cr₂O₃ - 0,01; Fe₂O₃ - 4,82; FeO - 6,38; CaO - 6,68; MgO - 4,25; MnO - 0,15; Na₂O - 6,14; K₂O - 4,70; P₂O₅ - 2,34; H₂O - 0,10; CO₂ - 0,004, were used. At the P-T parameters of the experiments, olivine doesn't melt, while the basaltic glass gives the melt with the composition, close to that of eclogite. The conditions of the conducted experiments and their results are given in the Table.

In all the experiments with the metal-silicate-carbon schist, the transformation of graphite into diamond, along with (except No 11) the growth of a diamond seed crystal, took place. Solid silicates and silicate melt (immiscible with the metallic one) have lower density and, due to the fact, were located in the upper part of the reaction volume. In the experiment with 20 % of basalt melt relative to the weight of metal, diamond seed crystal was blocked by silicate, so its growth did not occur. Diamond synthesis and growth of seed crystal did not take place in the experiment No 5 without metal. The last fact confirms the conclusions of the previous studies [1, 2], that at the pressures of 50-60 kbars and temperatures 1400-1500°C in the silicate-carbon melts, diamond doesn't form.

In the course of the experiments, initial olivine turned into pyroxene, garnet and newly formed olivine. The silicate melt of basaltic content at the end of the experiments crystallized into garnet and highly magnesian olivine and spinel, despite the apparent predominance of iron and nickel in the system. It was due to reductive conditions in the crystallization medium, at which transition metals concentrate themselves in a metallic phase.

In the synthesized diamonds, inclusions of metal, wustite and silicate phases (olivine and garnet) were established. Similar content of metallic and silicate inclusions was observed in the diamond crystal, synthesized in experiment No 1, though its formation proceeded in the medium with the content of silicate of only 1 % from the weight of the metal. The fact points to a selective incapture of silicate phases by diamond in the process of its crystallization.

Thus, the obtained results had shown, that in heterogeneous medium, consisting of metallic melt and solid or liquid silicate, diamond formation occurred at the same P-T parameters (50-60 kbars, 1400-1500°C), as in pure metal-carbon systems. That is, the presence of silicates doesn't reduce the chemical ability of

metallic melts to catalyze the transformation of graphite into diamond. Yet, silicates can block some parts of crystallization chambers, preventing the penetration of metallic melts there and, consequently, diamond formation. In the metal-silicate-carbon systems, along with diamond, olivine, garnet, pyroxene, spinel - i.e. the typical minerals of natural diamond-bearing parageneses, - crystallized.

Table. The conditions and results of the experiments on diamond crystallization in the metal-silicate-carbon systems

No of exp.	Silicate content in schist, wt. %	Experimental parameters			Diamond formation	
		P, kbars (± 2)	T, °C (± 20)	τ , hrs	Conversion of graphite into diamond	Diamond growth on seeds
1	Olivine – 1%	55	1450	40	Yes	Yes
2	Olivine – 2%	55	1500	40	Yes	Yes
3	Olivine – 5%	55	1500	60	Yes	Yes
4	Olivine – 15%	60	1450	70	Yes	Yes
5	Olivine – 100%	55	1500	70	No	No
6	Basalt – 2%	55	1500	60	Yes	Yes
7	Basalt – 4%	55	1500	70	Yes	Yes
8	Basalt – 4%	55	1550	90	Yes	Yes
9	Basalt – 10%	55	1500	70	Yes	Yes
10	Basalt – 17%	55	1550	90	Yes	Yes
11	Basalt – 20%	55	1500	65	Yes	No

References:

1. Chepurov A.I., Fedorov I.I., Sonin V.M. Experimental modeling of diamond formation processes. - Novosibirsk: NIC UIGGM SB RAS, 1997. - 197 p.
2. Chepurov A.I., Sonin V.M. On the crystallization of carbon in silicate and metal-silicate systems at high pressure // *Geologija i geofizika*. - 1987. - № 10. - P.78-81.

#Kosyakov V.I. *, Sinyakova E.F. ** The scheme of phase reactions in the Fe-FeS-NiS-Ni system

*ICh SB RAS, Novosibirsk, Prospect Lavrent`eva, 3, 630090, Russia

**IMP SB RAS, Prospect Akad. Koptuyug, 3, Novosibirsk, 630090, Russia

key words: [*Fe-Ni-S-system, pentlandite, the scheme of phase reactions*]

Two variants of Fe-Ni-S phase diagram, corresponding to two versions of pentlandite formation mechanism are recently presented. According to the first variant, pentlandite is formed by a peritectic reaction with participation of melt [1-4]. According to the second variant it occurs as a result of solid phase reaction [5-7]. Therefore, there is a problem to choose the only one variant, which is best suited to the whole set of the available experimental data on the study of the phase relations in the Fe-FeS-NiS-Ni system. We have critically analyzed the literature information and our own unpublished experimental data, referred to the temperature interval from 1200 to 430°C. It is stated that the occurrence of two versions is related to different interpretations of the data of microscopic study of the structure of the quenched samples, including the phases enriched in Ni: heazlewoodite, pentlandite, godlevskite, Ni-monosulfide solid solution. These phases appear as a

The authors wish to thank the Russian Foundation for Basic Researches (Project N 98-05-65314) for financial support of the work.

result of the decay reactions of heazlewoodite and godlevskite solid solutions, which are not preserved at quenching. This factor makes the reconstruction of the phase composition of the initial high-temperature samples difficult. Therefore, the results of microscopic studies of the samples, combined with the DTA and high-temperature X-ray data should be taken into account. Besides, to make the results of the analyses more reliable, it is worthwhile to make the system analysis of the whole set of experimental data and to construct the temperature sequence of the phase reactions in the Fe-FeS-NiS-Ni system.

It is shown that the first version of the pentlandite formation mechanism is based on the interpretation of small amount of the experimental information, related to the limited range of the compositions of the initial samples. The results, obtained by the authors of this version, allow, in our opinion, ambiguous interpretation and there is no sharply defined contradiction between them and the assumption on the solid phase mechanism of pentlandite formation. On the other hand, both the majority of the published data on isothermal sections and polythermal cross sections of the phase diagram and on physicochemical study of separate samples are in accordance with the second version of the pentlandite formation mechanism.

The scheme of the phase reactions in the Fe-FeS-NiS-Ni system is made using the data of Kullerud [5] on 9 isothermal sections of the phase diagram, our own previously published results, and also separate data from [1, 3]. To simplify this scheme we do not demonstrate the reactions with awaruite participation, which exists below 530°C. It should be noted that there are two versions of the phase diagram of Ni-S system. According to Rau [8], the existence area of $(\text{Fe}_x\text{Ni}_{1-x})_{3\pm y}\text{S}_2$ high temperature solid solution on the diagram is supposed to be single-phase. According to Lin [9], two solid solutions on the base of Ni_3S_2 and Ni_4S_3 are observed. More simple Rau's version of the phase diagram of the Ni-S system is used in the given study. Using the obtained results, the scheme of phase reactions, which considers the presence of two heazlewoodite solid solutions in this system, is not difficult to create. Fig. 1 demonstrates the scheme of phase reactions. We use the following designations of phases to

write the reactions: melt (L), monosulfide solid solution ($\text{Fe}_x\text{Ni}_{1-x}\text{S}_{1+y}$ (mss), Fe-Ni solid solution with the structure of γ -FeNi - taenite, FeNi - solid solution with the structure of α -Fe (α), triple heazlewoodite solid solution ($\text{Fe}_x\text{Ni}_{1-x}\text{S}_3$ (hzss), heazlewoodite Ni_3S_2 (hz), pentlandite solid solution ($\text{Fe}_x\text{Ni}_{1-x}\text{S}_8$ (pnss), godlevskite solid solution $\text{Ni}_{7+z}\text{S}_6$ (gdss), godlevskite Ni_9S_8 (gd). The equations of the phase

reactions in the studied system are written in the rectangular area of the scheme. The temperatures of these reactions ($^{\circ}\text{C}$) are given in parentheses. Phase associations disappear or appear on the phase diagram as a result of the reaction. The associations, which appear or disappear in binary boundary systems, are given in hexagonal areas. Similar associations, which appear or disappear in a triple system, are framed by ovals. The lines demonstrate the bonds between the phase reactions. If the represented scheme is supplemented by the schemes of the phase reactions in binary systems, the complete topological pattern of the phase diagram of the Fe-FeS-NiS-Ni system will be obtained. This type of schemes is widely used in reference books and data bases on the phase diagrams of the systems, formed from three chemical elements.

The represented version of the Fe-FeS-NiS-Ni system phase diagram correlates with all isothermal sections, plotted by Kullerud [5], besides the section at a temperature not much below 500°C . According to our data, the pnss+mss+gdss phase association, which is absent in Kullerud's work, exists in this section. Besides, we have used the data to refine Ni-S phase diagram in the area, where gdss converts into gd [10]. According to these data, at 500°C both phases are stable, whereas the diagram of Kullerud demonstrates only one gd-phase. Finally, according to Kullerud, at $T > 500^{\circ}\text{C}$, mss decays into two phases. We do not take into account this phenomenon as a two-phase $\text{mss}_1 + \text{mss}_2$ area is small

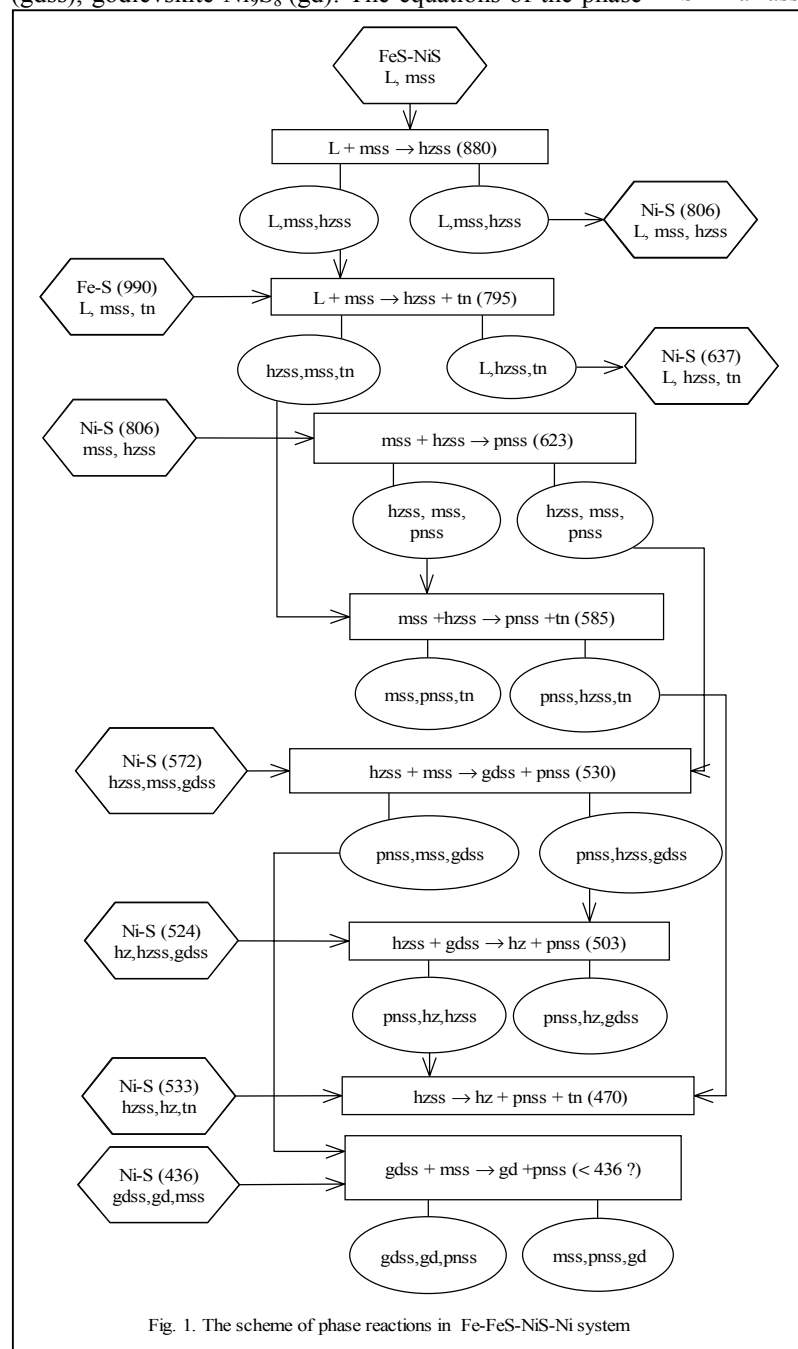


Fig. 1. The scheme of phase reactions in Fe-FeS-NiS-Ni system

Based on the phase diagram of binary boundary systems the scheme (Fig.1) can be used to define phase relations in the studied interval. The topological scheme of isothermal section of the diagram at 520°C is given in Fig.2 as an example.

The performed analysis of the phase relations in the Fe-FeS-NiS-Ni system evidences for solid phase mechanism of pentlandite formation. This conclusion is of vital importance to interpret the results of the study of natural samples of granular pentlandite and to describe its formation in the most Cu-depleted pyrrhotite ores.

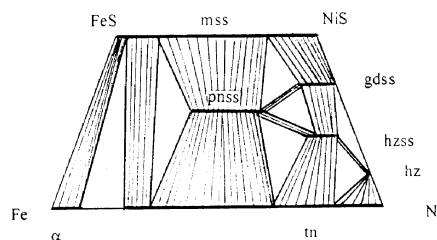


Fig.2. Scheme of phase ratios in isothermal cross section at 520°C

References:

- Misra K.C. & Fleet M.E. (1973) // Econ. Geol., V. 68, pp. 518-539.
- Distler V.V., Malevsky A.YU. & Laputina, I.P. (1977) // Geokhimiya N 11, pp. 1646-1658.
- Barker, W.W., & Parks, T.C. (1983) // C.S.I.R.O. Res.Review, pp. 58-59.
- Sugaki A. & Kitakaze A. (1998) // Amer. Mineralogist, V. 83, pp. 133-140.
- Kullerud G. In: Experimental petrology and mineralogy. Yb. Carnegie Inst. Wash., 62 (1962-1963). Nedra, 1969, pp. 138-155.
- Fedorova ZH.N. & Sinyakova .F. (1993) // Geologiya i Geofizika V34, N 2, pp. 84-92.

7. Karup-Moller, S, & Makovicky, E. (1995) // N.Jb.Miner.Mh., H. 1. pp.1-10.
8. Rau H.J. (1976) // J. Phys. Chem. Solids, V.37, pp. 929-930.
9. Lin R. Y., Hu D.C., Chang Y.A. (1978) // Met. Trans., V. 9B, N 4, pp. 531-538.
10. Stolen S., Fjellvag H., Gronvold F. et al.(1994) // J.Chem.Thermodynamics, V.26, pp. 987-1000.

Karzhavin V.K., Voloshina Z.M. Modelling of P–T parameters of phase equilibria

Geological Institute, Kola Science Centre RAS, Apatity

Thermodynamic studies are very important for the analysis of the processes, which are accompanied by chemical and phase transformations in the wide intervals of temperature and pressure. For equilibrium and locally equilibrium processes, a calculation of parameters of state allows to model relatively precisely the real conditions and to present information, which is difficult to obtain experimentally. It is widely accepted, that composition and thermodynamic properties of the equilibrium products unambiguously depend on bulk composition, temperature, and pressure [1]. An estimation of the parameters is also the major purpose of the reverse problem of chemical equilibrium. It allows to apply the thermodynamic methods for solution of some geological problems. Estimations of temperature and pressure of mineral formation is an important problem for prediction of the natural post-magmatic and metamorphic processes. In order to solve this problem, chemical compositions of coexisting minerals were analyzed with the “Cameca” microprobe, and the parameters were calculated on the basis of equilibrium constants. The equation $\ln K/dT = \Delta H/RT^2$ was used for determination of the dependence of the equilibrium constant on temperature at constant pressure. The dependence of the equilibrium constant on pressure at constant temperature is expressed by equation $\ln K/dP = \Delta V/RT$.

Application of unreliable information to determination of natural thermodynamic conditions can influence the reliability of results. At the traditional approach to calculations, only a part of chemical compounds participating in reactions is regarded. A correctness of a choice of components in the system would give a possibility to write all the reactions, which allow to get an objective information. In this connection, the TWQ is the

most attractive method, which allows to estimate an equilibrium in the system by means of comparison of position of all equilibria, which are possible in the system, and to calculate temperature and pressure using the data on chemical composition of all coexisting phases [2]. Based on the internally consistent thermodynamic database on chemical compounds, an automatic calculation can be done by the TWQ. The calculations are based on the following equations:

$$T = [\Delta H^0 + \Delta V^0(P-1)] / (\Delta S^0 - R \ln K) \text{ and}$$

$$T = (-RT \ln K - \Delta H^0 + T \Delta S^0) / \Delta V^0.$$

The equilibrium constants are calculated as a function of temperature and pressure. In the case of equilibrium in the given system, all calculated curves of reactions should intersect in one point on the PT field. In the given case, an equilibrium in the system is determined by phase and chemical compositions, while equations, which determine P, T, and compositions of equilibrium phases in the intersection point, could be obtained from the condition of equal chemical potentials of components in all phases. If the system is not in equilibrium, then the area of curve intersections forms in the PT field because of displacement of the curves. A size of this area is proportional to a deviation from equilibrium. The method allows to solve a reverse problem, i.e. to find out, whether an equilibrium exists in the studied object or system at given temperature and pressure. According to the above description, the present study is aimed at the estimation of possibilities of the TWQ method.

A basis for our study was a petrographic and microprobe investigation of mineral compositions. We intend to estimate conditions, which allow to solve a problem of determination of PT parameters of transformation of the studied natural object into metamorphic minerals in the presence of volatile components in the conditions of possible equilibrium. A metamorphic system as a complex natural system is considered as a result of evolving totality of diverse processes, which are in definite relationships. A sample of altered gabbro-norite (Panskaya intrusion, Kola Peninsular) was used as an example. Its mineral assemblage includes plagioclase, amphiboles, chlorite, clinozoisite. Chemical composition of the phases is shown in the table:

	SiO ₂	Al ₂ O ₃	FeO	MgO	CaO	Na ₂ O	K ₂ O
Amphibole	153.40	5.36	11.00	15.61	12.51	0.74	0.18
Amphibole	252.85	6.45	10.86	15.01	11.95	0.90	0.20
Clynozoisite	40.37	24.72	10.26	0.15	22.76	0.27	0.00
Plagioclase	55.58	28.30	0.00	0.00	10.38	5.74	0.00

The above material shows, that the studied system is composed of the following elements: Si, Al, Fe, Ca, Mg, Na, K, H, O. According to petrography, the following compounds were included into the system for the theoretical calculation at the initial stage: NaAlSi₃O₈ (albite), CaAl₂Si₂O₈ (anorthite), Ca₂Fe₅Si₈O₂₂(OH)₂ (actinolite), Ca₂Mg₅Si₈O₂₂(OH)₂ (tremolite), Ca₂Al₃Si₃O₁₂(OH) (clinozoisite), Ca₂FeAl₂Si₃O₁₂(OH) (epidote), Fe₃O₄ (magnetite), and SiO₂ (α-quartz). A combined database of the TWQ, which includes the data

from [3], was used as a source of thermodynamic values. The initial stage of the study regarded a “dry” variant of the mineral system. However, no chemical interactions were observed between the above components. A subsequent addition of volatile components, i.e. water, oxygen, and hydrogen to the system caused some chemical reactions, however estimation of PT parameters was impossible. A result of calculations for the system 1, which involves all volatile components, shows a presence of 11 chemical reactions, but an equilibrium is absent in

such a complex system (Fig. 1). The analysis of the results shows, that an absence of equilibrium in the system is conditioned by hydrogen-bearing reactions. A subsequent thermodynamic calculations in the absence of hydrogen showed, that remaining chemical compounds could be in equilibrium at $T = 404^{\circ}\text{C}$ and $P = 215 \text{ MPa}$. Seven reaction exist at these parameters. Their curves intersected in one point (numbers of reactions are shown on curves, Fig. 1):

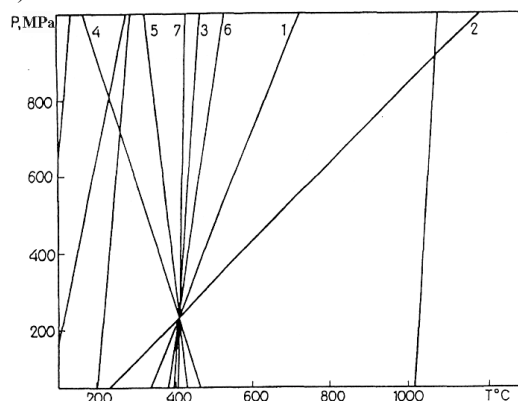


Fig.1. P-T diagram of chemical reactions in system 1.

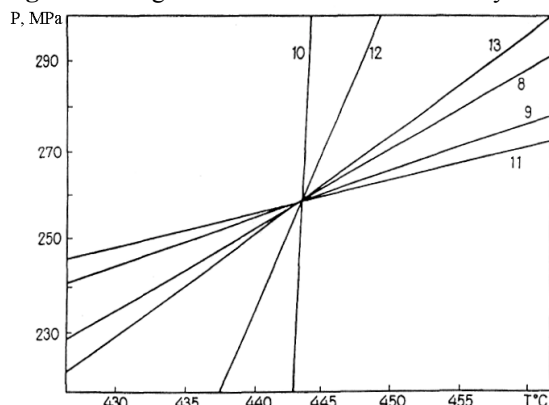
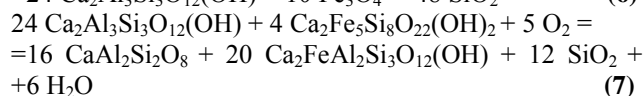
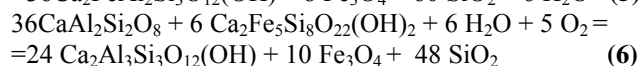
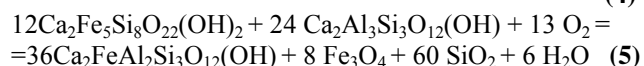
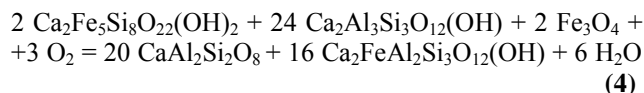
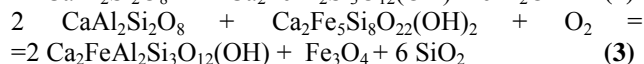
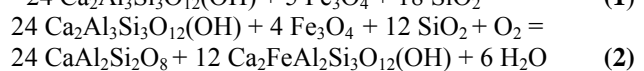
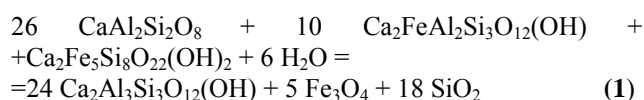
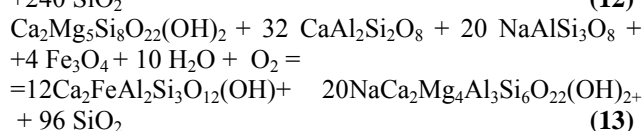
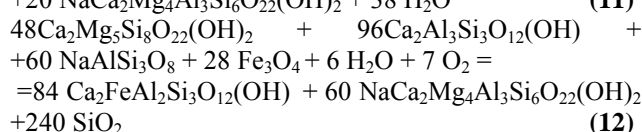
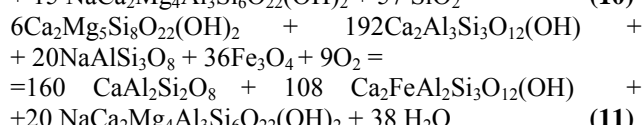
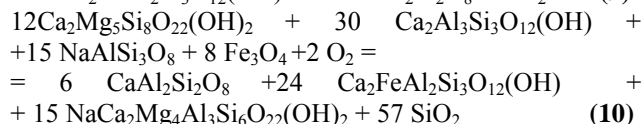
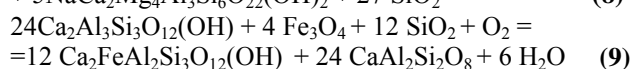
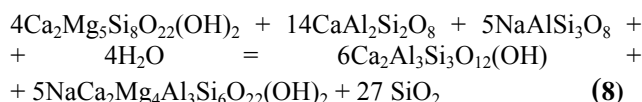


Fig.2. Estimation of P-T parameters in the natural sample according to equilibrium in system 2



An analysis of the reactions (1)-(7) shows the absence in them of Na and Mg-bearing compounds. That is a result of incorrect choice of chemical compounds participating in the reactions. Along with it, it should be noted, that chemical equilibrium expressed by reactions (1)-(7) could

be considered as real for the system with the given mineral compositions, but only in the absence of albite and tremolite. An attempt to add some Na and Mg-bearing compounds was undertaken. Na and Mg-bearing minerals, pargasite, magnesioriebeckite, edenite, and glaucophane, were added to the system separately or in pairs. Numerous variants of additional calculations showed, that any complication of the system caused its deviation from equilibrium. An equilibrium state, containing minerals of all above elements, was found in replacement of actinolite (actively participating in reactions 1, 3-7) to pargasite [$\text{NaCa}_2\text{Mg}_4\text{Al}_3\text{Si}_6\text{O}_{22}(\text{OH})_2$]. The thermodynamic calculations showed, that an equilibrium in the given system 2 is defined by the following chemical reactions:



Since pargasite is a high-temperature mineral, its appearance in the system caused a displacement of PT parameters to the high-temperature region. Reaction curves of the above chemical reaction intersected in one point at $T = 404^{\circ}\text{C}$ and $P = 215 \text{ MPa}$ (Fig. 2).

The above material showed possibilities of thermodynamic calculations and determination of equilibrium parameters using the chemical analysis. It should be noted, that reliable temperatures and pressures can be calculated in the case of a correct problem.

References:

- Zeldovich Ya. B. // Physical Chemistry Journal. 1938.V.11. Issue 5. P. 685.
- Berman R. G. // Can. Mineral. 1991.V. 29. N4. P. 833.
- Holland T. J. B., Powell R. // J. Metamorphic. Geol., 1990. V. 8 N1. P.89.

#Khranov D.A.,¹ Rusakov V.S.,² Eremin N.N.³ Structure and phase mechanisms of ilmenite

[#] This work is executed at the support RFFI, grant 98-05-64275.

and ferriilmenite oxidation in air: experimental and structural modeling

¹ Vernadsky Institute of Geochemistry and Analytical Chemistry Academy of Sciences, Moscow 117975, khramov@geokhi.ru;

² Department of Physics, Moscow State University, Moscow 119899, rusakov@moss.phys.msu.su;

³ Faculty of Geology-Crystallography and Chemistry, Moscow State University, Moscow 119899,

Study of mechanism of oxidation of ilmenite (FeTiO_3) is of essential interest for understanding the processes of the evolution of minerals and positions of inorganic materials. Experimental modeling of similar processes under the controlled T, P, $f\text{O}_2$ conditions allows to restore the picture of formation and following change of minerals. Besides, partly oxidized ($\approx 20\%$ Fe^{3+}) ilmenite (ferriilmenite) is referred to the class of new perspective magnetic materials concentrating the spin-echo glass (CC). Parameters of transition into the CC condition to a considerable extent are defined by the particularities of the system. So for correct understanding and prediction of magnetic characteristics such as CC it is necessary to know ion localization particularities of Fe^{3+} , as it defines the possible mechanisms of the frustration in the system.

I, %

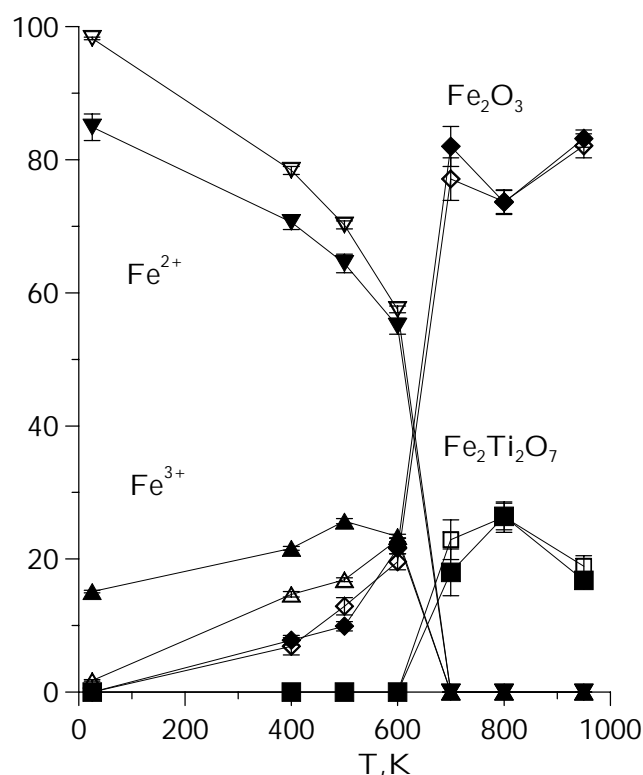


Fig.1 Changing the content of atoms of two- and trivalent iron in the structure of ilmenite (light badge) and ferriilmenite (dark badge). The correlation of phases Fe_2O_3 and $\text{Fe}_2\text{Ti}_2\text{O}_7$, formed in the system in the process of oxidation of the starting samples of FeTiO_3 and $\text{Fe}_{1.06}\text{Ti}_{0.94}\text{O}_3$.

In this work by the methods of Mossbauer spectroscopy (MS) of ^{57}Fe and computer structured modeling (KSM), we studied structural and phase mechanisms of oxidation in air ($T=400\text{--}950^\circ\text{C}$) of

ilmenite (FeTiO_3) and ferriilmenite samples with deficit of titanium $\text{Fe}_{1.06}\text{Ti}_{0.94}\text{O}_3$, synthesized at $T=1150^\circ\text{C}$ characteristic of running the magmatic processes and conditions of obtaining CC of the given type. It has been established that the process of ilmenite and ferriilmenite oxidation under $T = 400\text{--}600^\circ\text{C}$ proceeds in two parallel ways: 1) by the transition of Fe^{2+} ions into Fe^{3+} ones in the structure of a mineral; 2) by the separation of gematite and rutile phases in the amounts of $\approx 8\%$ (400°C) and $\approx 22\%$ (600°C). Based on the data on MC and structural modeling the following schemes of local charge compensations seem the most probable: $\text{Fe}^{2+} + \text{Ti}^{4+} \rightarrow \text{Fe}^{3+}(\text{Fe}) + \text{Fe}^{3+}(\text{Ti})$; $3\text{Fe}^{2+} \rightarrow 2\text{Fe}^{3+}(\text{Fe}) + \text{V}(\text{Fe})$. At the temperature of oxidation $T = 700^\circ\text{C}$ the structure of ilmenite completely disintegrates with formation of rutile, gematite and $\text{Fe}_2\text{Ti}_2\text{O}_7$ phases. The further increase of the oxidation temperature ($800\text{--}950^\circ\text{C}$) does not lead to the appearance of new phases, but only causes changes in their correlations.

Khodakovskiy I.L., Devina O.A., Sergeyeva E.I., Chernysheva I.V., and Priyomysheva M.N. A new edition of the "Handbook of thermodynamic data"

Vernadsky Institute of Geochemistry and Analytical Chemistry of the Russian Academy of Sciences, 117975 Moscow, Kosygin str., 19 "Dubna" University, Moscow Region, Dubna

key words: [*handbook, thermodynamic values, selection and consistency of the data, pure substances, chemical reactions, aqueous species, gas mixtures, solid solutions*]

The first edition of the "Handbook of Thermodynamic Data" by G.B.Naumov, B.N.Ryzhenko and I.L.Khodakovskiy was published in 1971[1] in former USSR. It was translated into English in USA in 1974 [2]. The Handbook was intended for use by the Earth scientists. Thermodynamic values for minerals and many other crystal substances as well as Gibbs formation energies for ions and undissociated molecules of a number of acids and dissolved gasses in aqueous solutions at temperatures up to 350°C provided thermodynamic calculation of equilibrium constants for a great number of reactions in hydrothermal systems.

The new edition summarizes the systematic work on the thermodynamic data selection and critical assessment performed by a number of researchers at Vernadsky Institute in cooperation with scientific research workers at other Institutes of RAS, and (during the last years) – in cooperation with "Dubna" University. Simultaneously with that work, experimental determinations of thermodynamic properties of a number of minerals and aqueous species (ions, as well as complex ions and molecules) were performed, using predominantly calorimetry and solubility methods. The results of those determinations were published in the papers. A part of those results were incorporated, as accepted values, in fundamental Handbook of the USSR Academia of sciences ("Thermal constants of substances" [3]), and in other reference books [4,5] as well.

It is expected that the Handbook will consist of three volumes. Each of these will involve several parts..

The first volume of the Handbook will incorporate *main results of experimental investigations* on thermodynamics of chemical systems: (1) inorganic and simplest organic individual substances, as well as chemical reactions in which these substances participate; (2) aqueous species (ions and complex ions and molecules as well); (3) binary aqueous solutions; (4) gas mixtures; (5) solid solutions.

The main sources of the data: 1. Hand-written card indexes on thermodynamic properties (were regularly kept up to 1985. A total of about 12 thousands of cards); 2. VINITI summary card indexes (from 1985 to 1994. About 10 thousand of cards); 3. The reprints collection; 4. Computer bibliography and experimental databases contained in the DiaNIK-win" system.

The Handbook will be the first one to systematize experimentally studied chemical systems and chemical reactions. This enables to not only perform local and global consistency procedures, but to use the feed-back principle as well for the algorithms of correlation and calculation of the equilibrium composition of multicomponent systems of any phase constitution.

The second volume will incorporate *accepted values and substantiation of their selection* for a number of chemical systems. The selection of the systems was due to the problems which were solved by the authors since 1963. These problems were solved within the framework of application of the chemical thermodynamics methods to investigations of conditions of the mineral formation in different natural and technogenic systems. Thermodynamic properties of pure inorganic and simple organic substances, chemical reactions, aqueous species (ions, complex ions and molecules), and binary aqueous solutions will be considered as well. The first part of the second volume of the Handbook will incorporate the results of analysis of published experimental data for one- and two-component chemical systems.

All accepted values are consistent with the international recommendations of CODATA, IUPAC, IAEA, and UE, and they are related to the recommendations of the fundamental reference books.

The third volume will incorporate the *tables of thermodynamic properties* of minerals and principal mineral-forming substances, including aqueous species, in large temperature and pressure ranges. The tables will be prepared in the "DiaNIK-win" computer system.

In 2001 the first parts of the mentioned volumes (incorporated thermodynamic information on one- and twocomponent systems) will be published. The parts incorporated the data on three-, four-, fivecomponent and more complicated systems are prepared in parallel.

References:

1. Naumov G.B., Ryzhenko B.N., Khodakovskiy I.L. Handbook of thermodynamic data. M.: Atomizdat. 1971. 240 pp.
2. Naumov, G.B.; Ryzhenko, B.N.; Khodakovskiy, I.L. Handbook of Thermodynamic Data (PB-226 722/7GA) (NTIS: Springfield, Va.), 1974. 373 pp.
3. Termicheskie konstanty veschestv. Pod red. V.P. Glushko. Vypuski III-X, M.: AN SSSR, 1968-1981.
4. Fuger J., Khodakovskiy I.L., Sergeev E.I., Medvedev V.A., Navratil J.D. The Chemical Thermodynamics of Actinide Elements and Compounds: Part 12. The Actinide Aqueous Inorganic Complexes; Vienna: International Atomic Energy Agency, 1992, 224 p.
5. CODATA International Geothermodynamic Tables. Editors: I.L.Khodakovskiy, E. F. Westrum, Jr. and B.S. Hemingway. 1995. 276 p.

Stolyarova T.A. The role of oxygen chemical potential in the thermodynamics of minerals of apatite group.

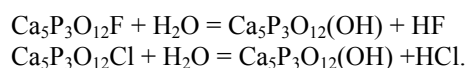
key words: [enthalpy, chemical potential, apatite]

The thermochemical study of minerals of apatite group has been carried out using the differential automatic microcalorimeter DAC1-1A adapted for the work in aggressive media. 20 wt% aqueous solution of hydrochloric acid (3.5 ml in volume, sample of 1-3 mg) has been used. Minerals were dissolved at 40°C (313.15 K). The results obtained have been recalculated to a standard enthalpy of mineral formation.

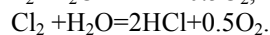
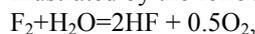
The thermodynamic values obtained for the synthesized apatite of stoichiometric composition and vitlokite are close to reference data [Robie et al., 1978]. They are given in table 1 alongside with the data on other minerals used in thermodynamic calculations. For the sake of convenience and immediate thermodynamic comparing the minerals, the values of standard enthalpy of mineral formation recalculated to one atom ($\Delta H_{0,298}$) and characterizing the averaged energy of bonds between atoms are also given in the table. In this value the minerals of apatite group form the following series: hydroxylapatite-chlorapatite-vitlokite-fluorapatite. Fluorapatite is shown to be the most stable chemical compound with especially strong bonds between atoms. This fact explains its universal occurrence in nature. However, the study of the chemical properties of natural fluorapatites discovered a common deficiency of fluorine in them relative to stoichiometric composition. We selected and thermochemically studied about a full series of apatites from fluorapatites with fluorine content close to theoretical one to practically fluorine-free phosphates close in composition to vitlokite.

The deficiency of volatiles is characteristic of all the natural apatites. The volatile contents in them are essentially lower than theoretical ones: 3.8, 6.8, and 1.8 wt% for fluor-, chlor-, and hydroxyl- apatites, respectively. This is related to the lack of calcium end members CaF_2 , CaCl_2 , and $\text{Ca}(\text{OH})_2$ which form solid solutions with phosphates close to vitlokite ($\text{Ca}_9\text{P}_6\text{O}_{24}$). High chemical affinity of these major apatite components is shown by reactions 1-3 in table 2. These data as well as $\Delta H_{0,298}$ value set fluorapatite, which is characterized by particularly strong chemical bonds of CaF_2 with phosphate component, apart from the apatite series.

The equilibria between apatites of different types are conveniently modeled by simple exchange reactions:
 $\text{Ca}_5\text{P}_3\text{O}_{12}\text{F} + \text{HCl} = \text{Ca}_5\text{P}_3\text{O}_{12}\text{Cl} + \text{HF}$



However, these reactions only seem simple because chemical activity of the participating in them acidic components of the solutions (HF, HCl) depends on many factors and first of all on the redox regime. This is clearly illustrated by the following reactions:



The fluid components F_2 , Cl_2 , O_2 participating in them play a significant part in thermodynamic calculations because they represent a reference state of the substance with zero values of enthalpy and free formation energy ($\Delta H_{0298}=0$, $\Delta G_{0298}=0$). The calculations of apatite equilibria (reactions 4-5 in table 2) discover the complicated thermodynamic relationships between apatite varieties which are governed by temperature, pressure, and geochemical factors. The major factors such as chemical potentials of fluorine, chlorine, and water are responsible for the formation of fluor-, chlor-, and hydroxyl- apatites, respectively, the chemical potential of oxygen in many respects governs the equilibria of fluor(chlor) apatites with hydroxylapatites (reactions 5,6 in table 2):

$$\Delta G_{0T} = \mu_{\text{H}_2\text{O}} + 0.5\mu_{\text{O}_2} - \mu_{\text{F}_2(\text{Cl}_2)}.$$

This factor should be taken into account when plotting phase diagrams of apatites. The diagram of chemical potentials of fluorine and chlorine presented in fig. 1 is of major importance. It corresponds to the standard water pressure ($P_{\text{H}_2\text{O}}=1$ atm, $\mu_{\text{H}_2\text{O}}=0$) and chemical potential of oxygen corresponding to the redox buffer $2\text{NiO}=2\text{Ni}+\text{O}_2$, $\Delta G_{0T}=-\mu_{\text{O}_2}=-423.16$ kJ $T=298\text{K}$) and -298.44 kJ ($T=1000\text{K}$).

The narrowed stability field of hydroxylapatite on the diagram corresponds to the standard water pressure. It should expand with fluid pressure and oxygen fugacity. However, the diagram is well representative of the thermodynamics of minerals of apatite group. The major mineral in this group is fluorapatite which shows a very high affinity to fluorine and appears at very low chemical potential of the latter in solutions. As it is seen on the diagram, the stability field of fluorapatite expands with temperature due to the narrowing of the stability field of chlorapatite. The reverse relationships are observed for hydroxylapatite: it tends to replace fluorapatite and particularly chlorapatite with increasing temperature. But its distribution is limited by fluid (water) pressure and redox conditions (oxygen chemical potential).

The regular thermodynamic relationships of the major apatite varieties presented on the diagram (fig.1) reflect the common peculiarities of halide-oxide equilibria enclosing simple calcium compounds entering their composition as end members. Presented on the diagram of fluorine and chlorine chemical potentials (fig.2) are oxides, hydroxides, calcium fluorides and chlorides. These simple compounds are representative of the same thermodynamic regularities characteristic of hydroxide-halide systems as complex phosphate compounds represented by fluor-, chlor-, and hydroxyl-apatite varieties.

Oxygen chemical potential is used in thermodynamic models when metals of variable valence are present in the systems. In the above buffer equilibria they are iron and nickel (reactions 12 and 13 in table 2). However, the

elements of apatite equilibria are of constant valence and the effect of oxygen chemical potential is due to the specific of halide systems. Let us consider in a simplified form the effect of oxygen chemical potential on apatite equilibria at the fixed standard values of chemical potentials of fluorine and chlorine at 298 and 1000 K. At these conditions chemical potentials of oxygen and water corresponding to minerals 5 and 6 in table 2 obey a simple dependence $\mu_{\text{H}_2\text{O}}=-0.5\mu_{\text{O}_2}$ determining the stability fields of hydroxylapatites on the diagram (fig.3) relative to redox buffers $2\text{NiO}=\text{Ni}+\text{O}_2$ and $2\text{Fe}_3\text{O}_4+3\text{SiO}_2=3\text{Fe}_2\text{SiO}_4+\text{O}_2$ $\Delta G_{0T}=-\mu_{\text{O}_2}=-456$ kJ (298 K) and -316 kJ (1000 K). The diagram illustrates the expansion of the stability field of hydroxylapatite relative to fluor- and chlor-apatites with increasing temperature.

The effect of the redox conditions on apatite equilibria is observed at comparing Earth's rocks with Moon's rocks and meteorites in which hydroxylapatites are absent due to the low chemical potential of oxygen. Chlor- and fluorapatites in them associate with vitloquite as well as with alkaline phosphates which are absent in the Earth's rocks and have a high solubility in an aqueous phase.

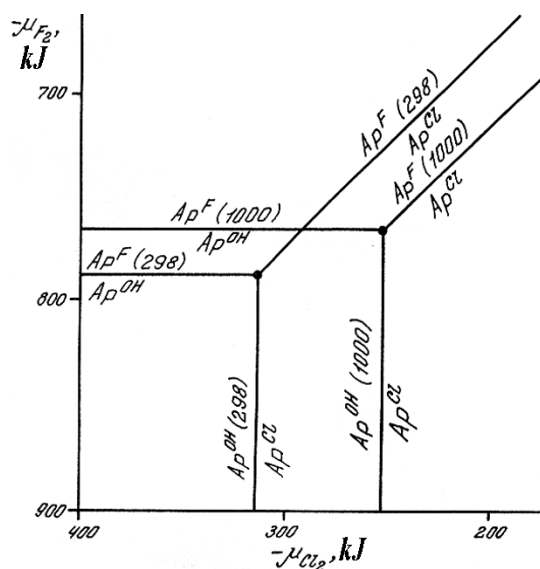


Fig. 1. Isotherm of fluor-, chlor-, and hydroxylapatites (298 K, 1000 K) on the diagram of chemical potentials of fluorine and chlorine at standard water pressure ($P_{\text{H}_2\text{O}}=1$ atm) under redox conditions corresponding to the Ni-NiO buffer

Table 1. Enthalpy and free energy of mineral formation (kj)

Mineral formulae and symbols	$-\Delta H_{298}^A$	$-\Delta H_{298}^o$	$-\Delta G_T^o$	
			298 K	1000 K
Ca ₅ (PO ₄) ₃ F (Ap ^F)	327.25	6872.20*	6508.12	5684.10
Ca ₅ (PO ₄) ₃ Cl (Ap ^{Cl})	315.72	6630.15*	6271.47	5426.52
Ca ₅ (PO ₄) ₃ OH (Ap ^{OH})	305.53	6721.60*	6338.43	6471.66
Ca ₉ P ₆ O ₂₄ (Wh)	316.99	12362.46*	11686.96	10156.67
CaF ₂	409.75	1229.26	1176.92	1060.49
CaCl ₂	265.27	795.80	748.06	642.12
Ca(OH) ₂	197.22	986.09	898.41	691.14
H ₂ O	95.28	285.83	237.14	129.56
NiO	119.87	239.74	211.58	149.22
Fe ₃ O ₄ (Mt)	159.39	1115.73	1012.73	789.43
Fe ₂ SiO ₄ (Fay)	211.34	1479.36	1379.38	1150.82
SiO ₂ (Q)	303.57	910.70	856.29	729.98

Note. ΔH_{298}^A - standard formation enthalpy recalculated to one atom; * ΔH_{298}^o values have been obtained experimentally by the authors.

Table 2. Thermodynamic characteristics of the reactions between the minerals of apatite group and simple chemical compounds (kj, T, K)

NN	Reactions	ΔH_{298}^o	ΔG_{298}^o	ΔG_{1000}^o
1	Wh + CaF ₂ = 2 Ap ^F	-152.78	-149.42	-151.09
2	Wh + CaCl ₂ = 2 Ap ^{Cl}	-102.08	-107.95	-54.28
3	Wh + Ca(OH) ₂ = 2Ap ^{OH}	-94.90	-93.04	-94.99
4	2Ap ^F + Cl ₂ = 2Ap ^{Cl} + F ₂	483.44	472.68	514.62
5	2Ap ^F + H ₂ O + 0,5O ₂ = 2Ap ^{OH} + F ₂	587.12	575.27	617.41
6	2Ap ^{Cl} + H ₂ O + 0,5O ₂ = 2Ap ^{OH} + Cl ₂	103.68	102.59	102.79
7	CaF ₂ + Cl ₂ = CaCl ₂ + F ₂	433.44	428.83	418.35
8	CaF ₂ + H ₂ O = Ca(OH) ₂ + F ₂	699.26	516.51	561.85
9	CaCl ₂ + H ₂ O + 0,5O ₂ = Ca(OH) ₂ + Cl ₂	96.50	87.68	143.50
10	CaF ₂ = Ca + F ₂	1229.20	1176.86	1060.44
11	CaCl ₂ = Ca + Cl ₂	795.76	748.03	642.09
12	2NiO = 2Ni + O ₂	479.48	423.16	298.44
13	2Mt + 3Q = 3Fay + O ₂	525.48	456.18	316.36

Note. For the symbols of minerals see table 1.

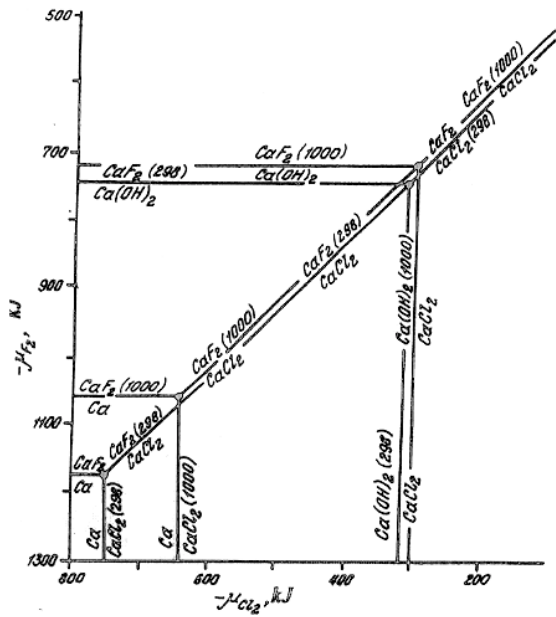


Fig. 2. Diagram of chemical potentials of fluorine and chlorine hydroxides, calcium fluorides and chlorides.

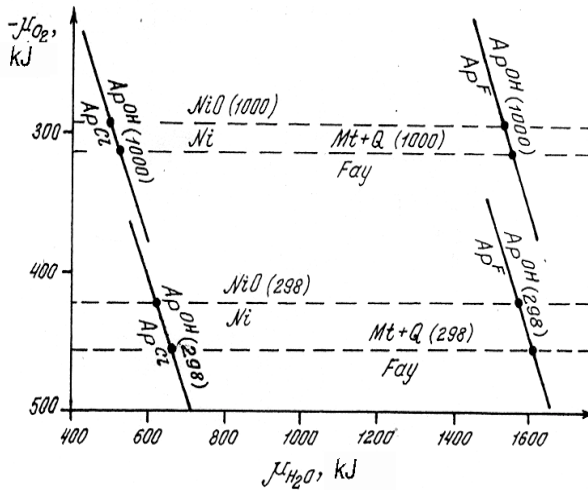


Fig. 3. Stability fields of hydroxylapatite at T= 298 K and 1000 K on the diagram of chemical potentials of oxygen and water under conditions corresponding to the nonvariant points $\mu_{F_2}-\mu_{Cl_2}$ (see fig.2) of calcium fluorides and chlorides.